

Power Quality Analysis in Electric Traction System with Three-phase Induction Motors

B. Milešević, I. Uglešić, B. Filipović-Grčić

Abstract—Three-phase induction motors are widely used in electric traction systems. Impacts of the traction vehicle equipped by three-phase induction motors on power quality are much different from the impacts of vehicles with DC traction motors. In this paper, the effects of the traction vehicle operation with three-phase induction motors on power quality in 110 kV transmission network are investigated.

The electric traction system 25 kV, 50 Hz and the traction vehicle with 3f induction motors were modeled including AC/DC rectifier and DC/AC inverter based on IGBT technology. The parameters of those power electronic elements directly determine the current and voltage waveforms and power quality parameters.

Modeling, measurements and analysis of power quality parameters were presented. Three operation modes of traction vehicle were considered including acceleration, constant drive and regenerative braking. During the test drives, the values of total harmonic distortion, unbalance, flicker and power factor were obtained.

Keywords: electric railway, power quality, induction motors.

I. INTRODUCTION

ELECTRIC railway system is essential for the transport of people and goods. Numerous advantages of electric railway have been proven in comparison with other forms of transport, from reliability and safety to the speed and comfort [1]. The development of societies and economics entails the improvement of railways. The most important railway transportation routes are electrified which makes this system more competitive and environmentally more acceptable [2].

Electric railway is a single phase consumer [3]. Operation of traction vehicle may cause significant effects on power quality parameters in the power system [4]. One of the most widely used railway electrification systems is 25 kV, 50 Hz. This system is powered from the electric power transmission system and it supplies traction vehicles through contact network. Voltage and current waveforms in the railway system directly depend on the type of traction vehicle, its characteristics and electrical properties [5]. Electric traction

vehicles are commonly equipped by DC motors or 3f AC motors [6]. The advantages of 3f induction motors are manifested in possibilities of energy recovery during braking or operating on downhill and simplest maintenance. Electric railway system have an influence on systems that ensure reliability of the system (communication subsystem), but also on the systems in the vicinity which are sensitive to disturbances [5], [7], [8]. Different traction vehicle supply current and voltage effect with different disturbances.

Power transformer at traction vehicle is connected to AC/DC rectifier which is connected to DC link (Fig. 1 and Fig. 2). DC voltage is converted by DC/AC inverter to 3f AC voltage and supply 3f AC induction motor. Power electronics elements, rectifier and inverter, are performed by thyristors or IGBT [9].

All measurements were performed during acceleration, constant drive and regenerative braking of electric traction vehicle. Waveforms of electric parameters in different operation modes are compared and deviations from nominal values are found according to the applicable standards [10], [11]. The measurement and analysis of power quality parameters in traction substation during the operation of locomotive equipped with 3f induction motors were presented.

II. OPERATION OF TRACTION VEHICLES WITH 3f INDUCTION MOTORS IN ELECTRIC RAILWAY SYSTEM 25 kV, 50 Hz

The operation of the single phase 25 kV (50 Hz) electric traction system is significantly different from the electric power system which supplies it [3].

The electric traction system is supplied from electric power system through power transformers located at traction substation. These transformers are connected to two phases of the power transmission system. Traction power supply network is separated by neutral section to the independent sections which are supplied from different traction substations. Fig. 1 shows a principle connection scheme of the 25 kV, 50 Hz electric traction system to 110 kV transmission network.

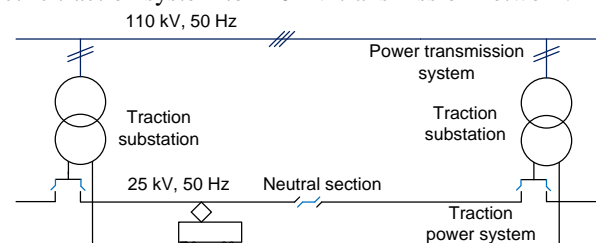


Fig. 1. Electric traction system

This work has been supported in part by the Croatian Science Foundation under the project “Development of advanced high voltage systems by application of new information and communication technologies” (DAHVAT).

B. Milešević, I. Uglešić and B. Filipović-Grčić are with the University of Zagreb, Faculty of Electrical Engineering and Computing, Unska 3, Zagreb, Croatia (e-mail of corresponding author: bosko.milesevice@fer.hr).

Electric traction vehicles are powered from contact network via pantograph and power transformer that adjust the 25 kV voltage to suitable value for induction traction motors (Fig. 2).

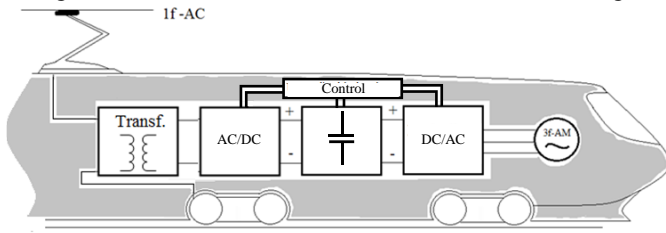


Fig. 2. Electric traction vehicle with induction motor

In this paper, multi-system traction vehicle supplied by 25 kV, 50 Hz system was used. The nominal drive power of one unit is 6.4 MW and heating power is 900 kVA [12], [13]. In Fig. 3 the measured effective values of current and active/reactive power on 25 kV side are shown. The values of

current and power change stepwise and depend on the operation mode. The measured supply current exceeded 300 A, while at the same moment the maximum measured active and reactive powers were 7.5 MW and 950 kvar, respectively. The measured reactive power had a permanent positive sign, whereas active power changed both positive and negative sign, depending on power flow direction. In the periods when the value of active power is positive, energy flows from power substation to a traction vehicle while a negative sign indicates the opposite flow of energy. Maximum active power during recuperation braking (energy recovery) was 5.5 MW and has been reached at the moment when the current was 215 A and reactive power was 440 kvar. As expected, the maximum power that can be recovered was less than the maximum power that the vehicle used for the acceleration.

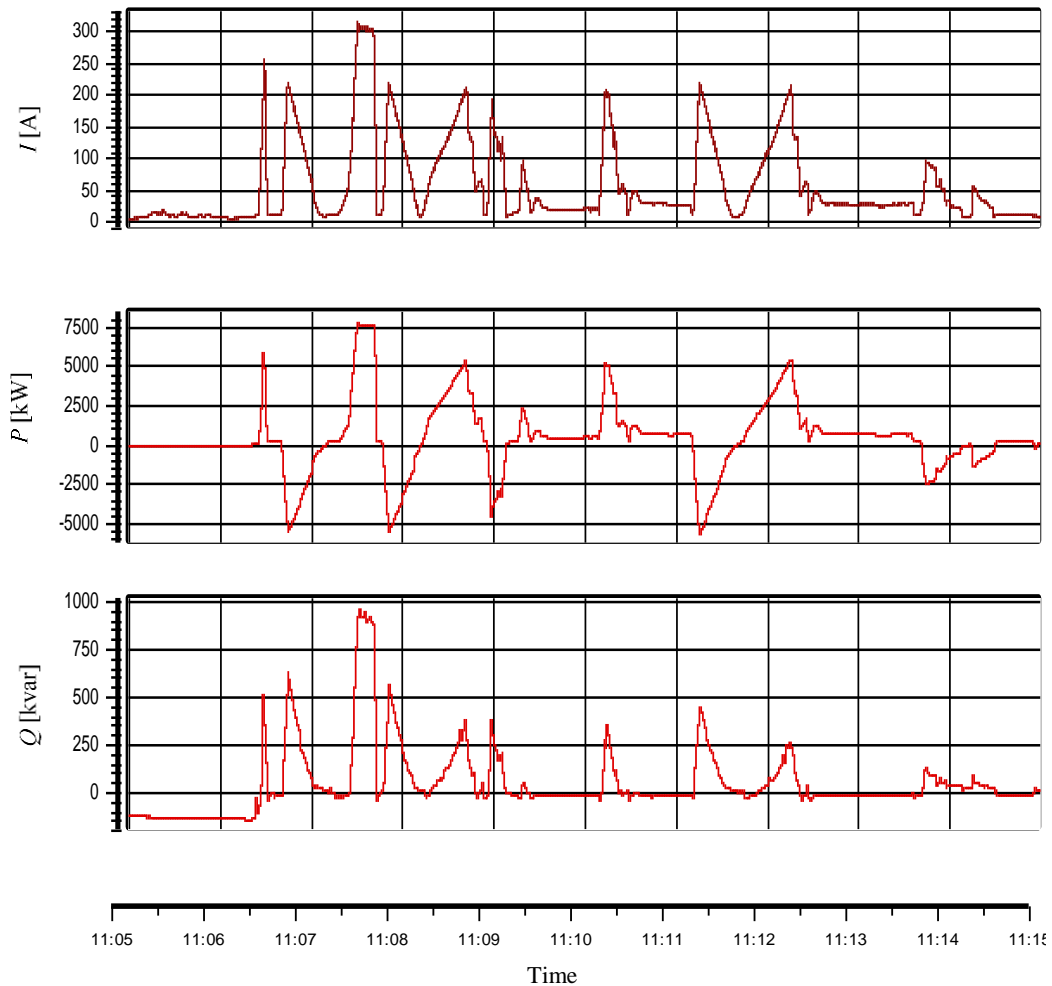


Fig. 3. Current, active and reactive power of electric traction vehicle with induction motors

III. MODEL OF TRACTION VEHICLE WITH INDUCTION MOTORS

The model of electric multiple unit of 2 MW continuous power was developed in ATP software and it includes power transformer at substation and on vehicle, IGBT converters, DC link and induction motor with rated power 525 kW.

The impedance of 110/25 kV power transformer referred to 110 kV side is $R=0.5 \Omega$ and $L=4 \text{ mH}$ (7.5 MW, $u_{k\%}=10\%$). Contact network impedance is $0.181+j0.447 \Omega/\text{km}$. DC link was modeled by capacitance ($C=36 \text{ mF}$) and inductance ($L=0.007 \text{ mH}$). Electrical scheme and model for calculation are shown in Fig. 4 and Fig. 5.

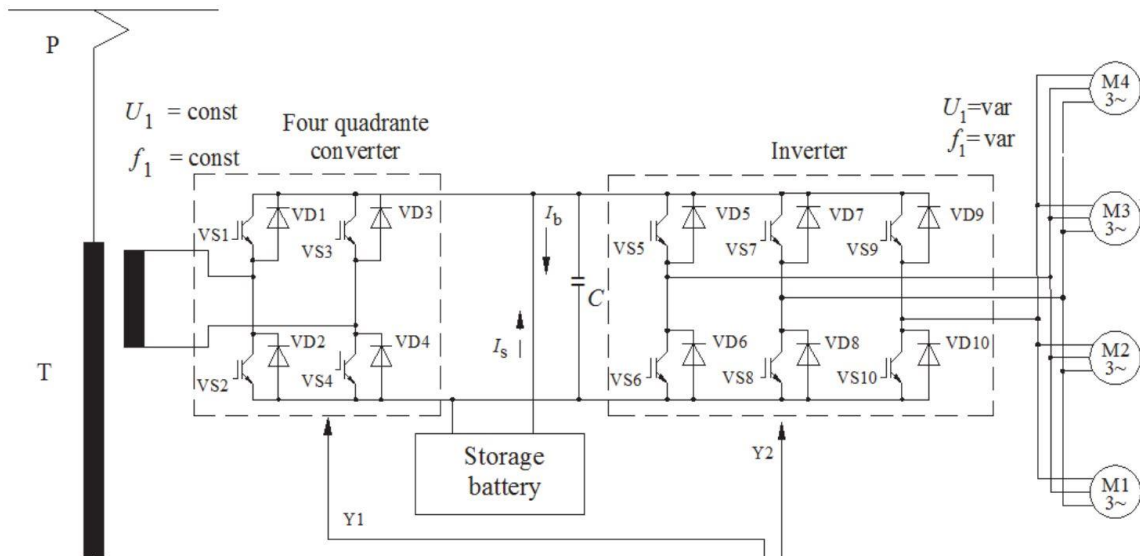


Fig. 4. Electrical scheme of traction vehicle with induction motors [14]

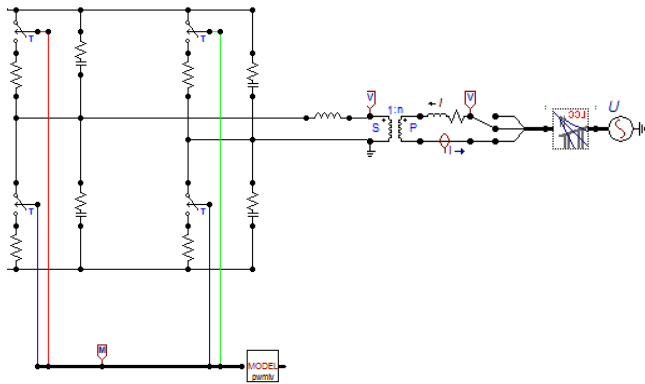


Fig. 5. Model for calculation in ATP

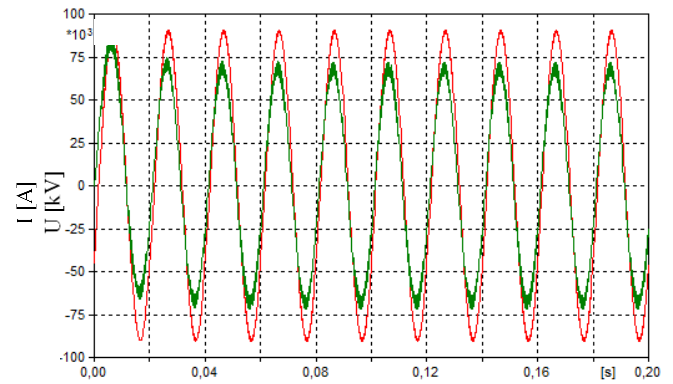


Fig. 6. Current (green) and voltage (red) on contact network on 110 kV side

Rectifier consists of four switches controlled by PWM (Pulse-Width Modulation) signal. The algorithm which generates the control PWM signals contains the modulation signals and carrier signal (triangular wave). The triangular signal was modeled and its frequency is an odd multiple of modulation signal. The frequency of the input signal is determined by the frequency of the contact network.

Inverter contains three branches each with two switches. The control of switches operation is realized by PWM module. The developed model of traction vehicle enables the analysis of any motor operation frequency. The current and voltage waveforms on 110 kV side of traction substation at the frequency 50 Hz are shown in Fig. 6. Current value is multiplied by factor 10.

These waveforms show that fundamental power frequency of 50 Hz is supplemented by some higher harmonics. FFT (Fast Fourier Transformation) is calculated for obtained voltage and current form (Fig. 7, 8 and 9) in order to analyse the power quality parameters.

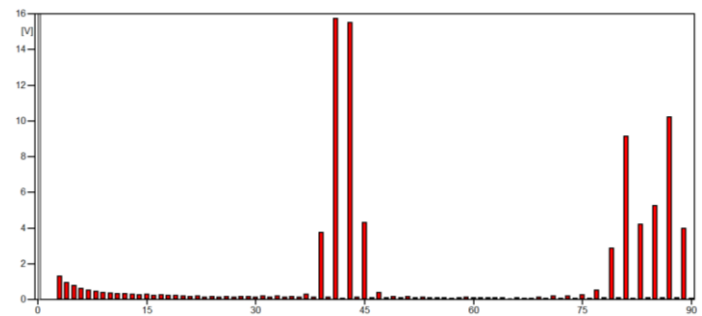


Fig. 7. Voltage FFT on 25 kV side (harmonics 3rd to 90th of power frequency)

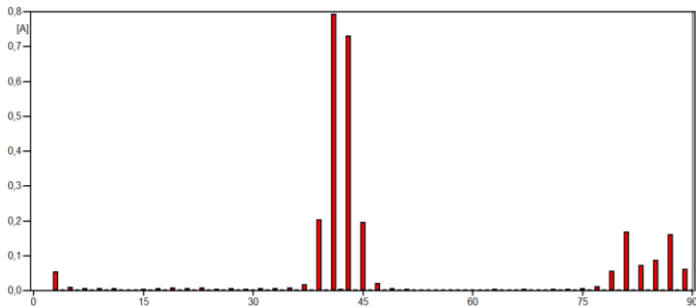


Fig. 8. Current FFT on 25 kV side (harmonics 3rd to 90th of power frequency)

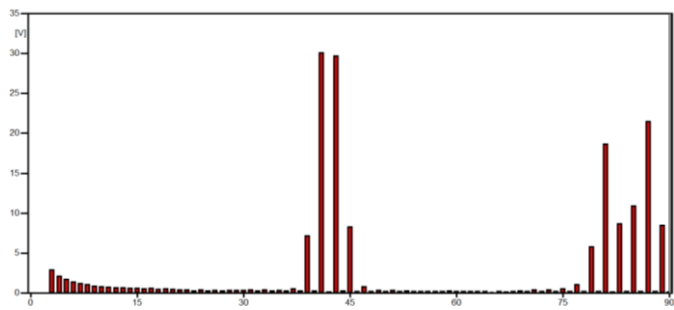


Fig. 9. Voltage FFT on 110 kV side (harmonics 3rd to 90th of pow. frequency)

The results depicted in figures 7 – 9 show that from all higher harmonics the 41st harmonic had a maximal magnitude of 30 V on 110 kV side which is about 0.03% of the magnitude of fundamental harmonic. The same harmonic on 25 kV side reached 16 V or 0.04% of fundamental harmonic. Also, the maximal higher harmonic of the current was 41st, with magnitude of 2.7% of fundamental harmonic.

IV. MEASUREMENT AND ANALYSIS OF VOLTAGE AND CURRENT WAVEFORMS

The measurements of power quality parameters were performed on 110 kV side in electric traction substation. Switching arrangement of substation and locomotive position during the measurements are shown in Fig. 10.

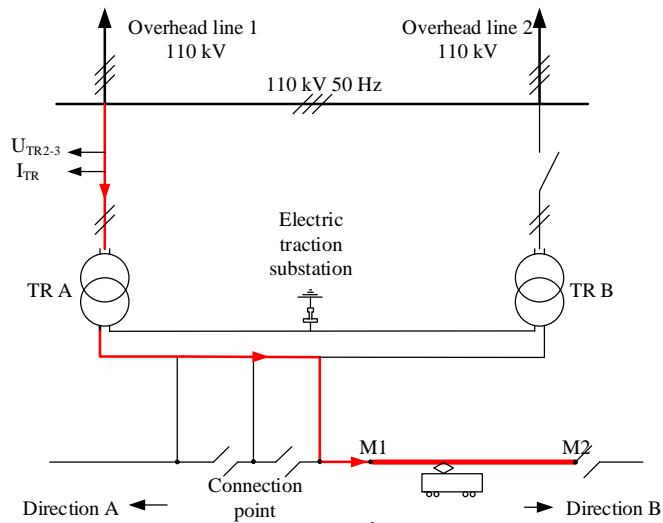


Fig. 10. Electric traction substation connection and train position

Two 110 kV overhead lines are connected to traction substation. The transmission and traction systems are connected via power transformers 110/25 kV with nominal power 7.5 MVA. During the measurements only transformer A was in operation. The one locomotive travelled from point M1 to point M2 on the section B.

Supply and regenerative current and voltage between phases L2 and L3 on 110 kV side were measured in the transformer bay. Also, the values of power factor, unbalance and total harmonic distortion (THD) were observed.

In this chapter the waveforms of voltage and current are presented. The waveforms depend on the operation mode (acceleration, constant drive or regenerative braking). Results are presented for all three operation modes. Also, the comparison tables with a content of each harmonic are given.

A. Voltage and current during the acceleration

The voltage and current waveforms during acceleration are presented in Fig. 11. Phase shift between voltage and current is very low. Figs. 12 and 13 show harmonic spectrum of those waveforms obtained by FFT.

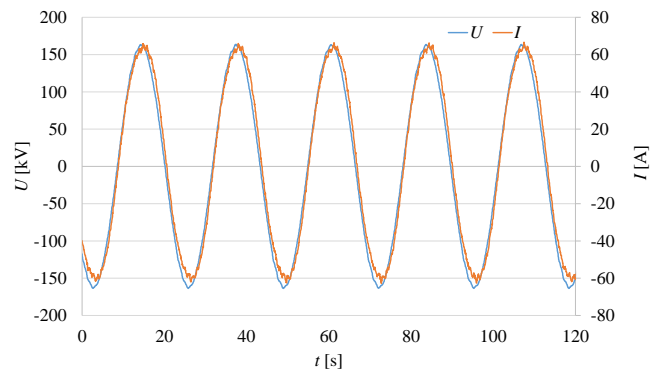


Fig. 11. Voltage and current through power transformer during the acceleration

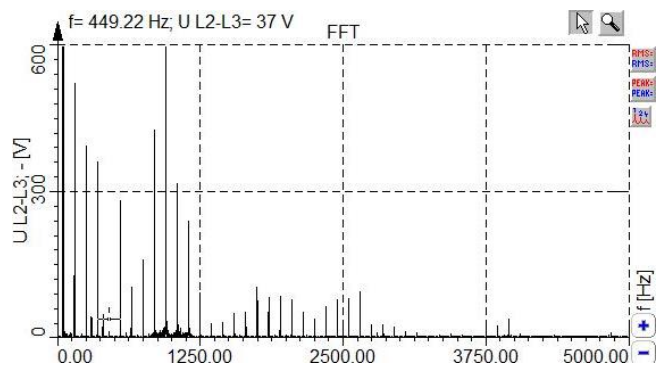


Fig. 12. FFT of voltage during the acceleration

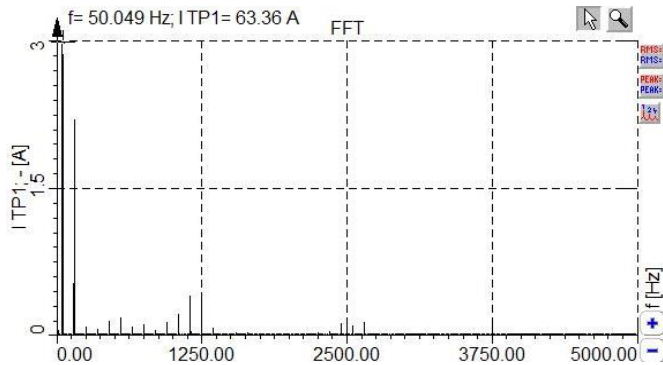


Fig. 13. FFT of current during the acceleration

B. Voltage and current during the constant drive

Voltage and current waveforms in constant drive operation mode are depicted in Fig. 14. Similarly as in the case of acceleration mode, phase shift is very low. FFT of obtained waveforms are presented in Fig. 15 and Fig. 16.

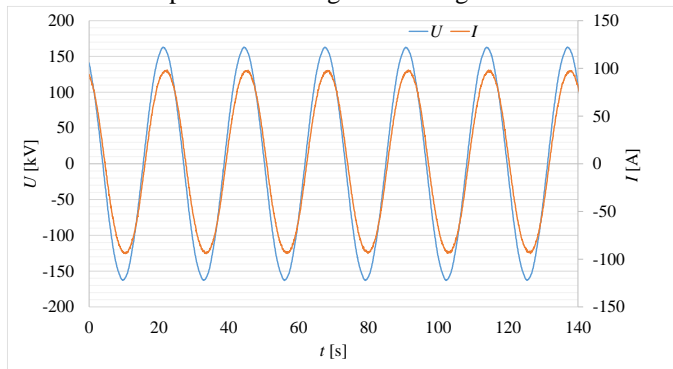


Fig. 14. Voltage and current during the constant drive

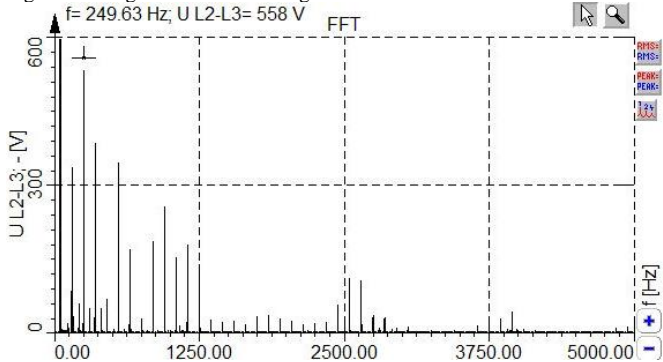


Fig. 15. FFT of voltage during the constant drive

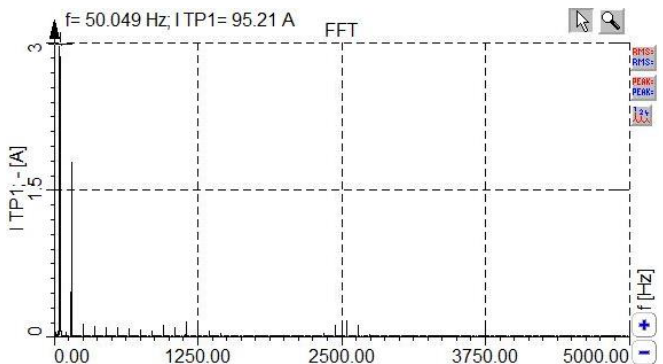


Fig. 16. FFT of current during the constant drive

C. Voltage and current during the regenerative braking

In operation mode of regenerative braking (energy recovery) phase the shift between voltage and current was 180° . In Fig. 17, waveforms of voltage and current flowing through power transformer are shown. Voltage had almost ideal sinusoidal waveform, but the current contained higher harmonics of significant magnitude. FFT up to 100^{th} harmonic of power frequency is shown in Figs. 18 and 19.

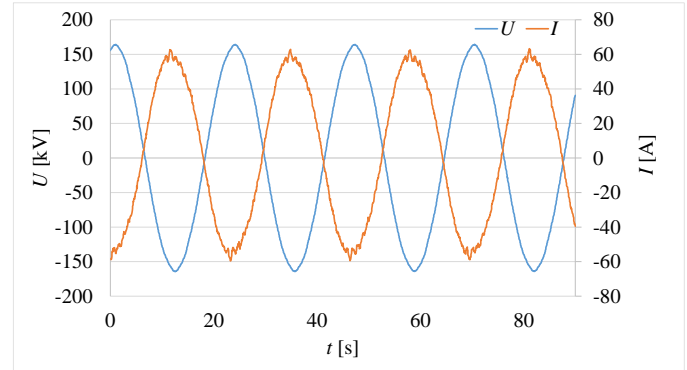


Fig. 17. Voltage and current during the regenerative braking

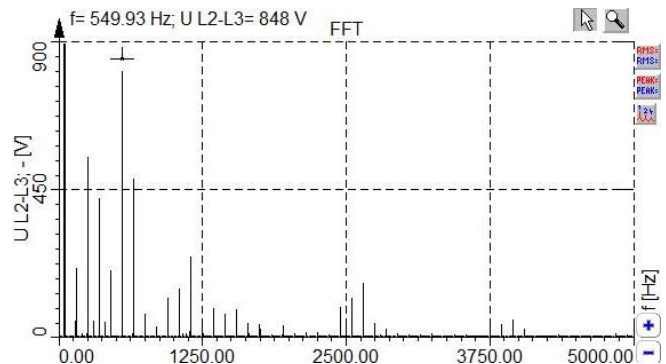


Fig. 18. FFT of voltage during the regenerative braking

In Table I the magnitudes of each voltage harmonic depending on all three operation modes are given, with regard to previous figures.

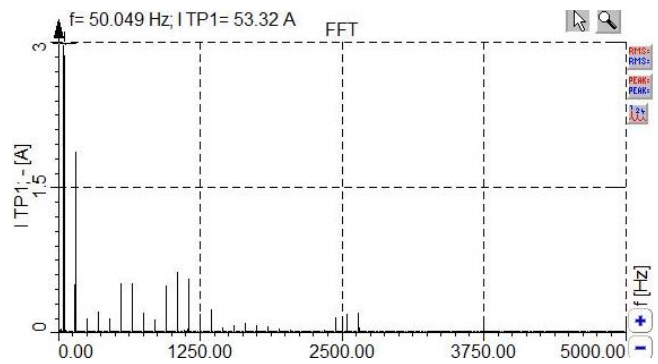


Fig. 19. FFT of current during the regenerative braking

Measured voltage had significant content of higher harmonics in all operation modes. Fig. 20 shows voltage THD in all phases on 110 kV side. THD of line voltage connected to power transformer reached 1.35%. The maximal values of THD were observed in acceleration and braking periods. In

phase L1, which is not connected to railway system, THD had almost constant value of 0.7%. This fact shows that electric railway vehicles equipped by 3f induction motors have an important effect on voltage waveform. However, the results presented in this paper were much lower than the values allowable in standards.

TABLE I
MAGNITUDE OF VOLTAGE HARMONICS DEPENDING ON OPERATION MODE

harmonic order v	Operation mode magnitude [%]		
	acceleration	constant drive	recuperation
1	100.00	100.00	100.00
3	0.31	0.20	0.13
5	0.26	0.37	0.34
7	0.25	0.22	0.28
9	0.12	0.02	0.13
11	0.28	0.19	0.53
13	0.03	0.13	0.30
15	0.12	0.01	0.05
17	0.29	0.05	0.02
19	0.26	0.03	0.08
21	0.10	0.02	0.09
23	0.11	0.10	0.16
25	0.05	0.05	0.04
27	0.03	<0.02	0.06
29	0.02	<0.02	0.04
35	0.03	<0.02	0.05
39	0.48	<0.02	<0.02
41	0.05	<0.02	<0.02
43	0.03	<0.02	<0.02
45	0.03	<0.02	<0.02
47	0.05	<0.02	<0.02
49	0.05	0.04	0.06
51	0.05	0.07	0.08
53	0.07	0.06	0.10

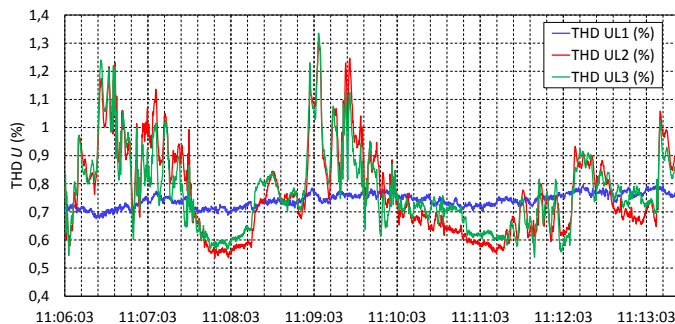


Fig. 20. Voltage total harmonic distortion on 110 kV side

In Table II, the magnitudes of each current harmonic in all three operation modes are given according to the values depicted in the before.

TABLE II
MAGNITUDE OF CURRENT HARMONICS DEPENDING ON OPERATION MODE

harmonic order v	Operation mode magnitude [%]		
	acceleration	constant drive	recuperation
1	100.00	100.00	100.00
3	3.71	1.88	3.54
5	0.15	0.14	0.28
7	0.10	0.12	0.43
9	0.26	0.13	0.30
11	0.22	0.11	0.98
13	0.22	0.09	1.00
15	0.17	0.09	0.41
17	0.20	0.04	0.24
19	0.36	0.06	0.92
21	0.15	0.09	1.20
23	<0.10	0.39	1.09
25	0.61	0.19	0.34
27	0.24	0.07	0.45
29	0.10	<0.10	<0.10
35	<0.10	<0.10	<0.10
39	<0.10	<0.10	<0.10
41	<0.10	<0.10	<0.10
43	<0.10	<0.10	<0.10
45	<0.10	<0.10	<0.10
47	<0.10	<0.10	<0.10
49	0.22	0.03	0.30
51	0.22	0.19	0.38
53	0.26	0.12	0.40

The measured current had significant content of higher harmonics in all operation modes. The value of current THD in all three phases on 110 kV side is presented in Fig. 21. THD of current flowing through power transformer reached 2.7%. Maximal values of THD were observed during acceleration and braking periods.

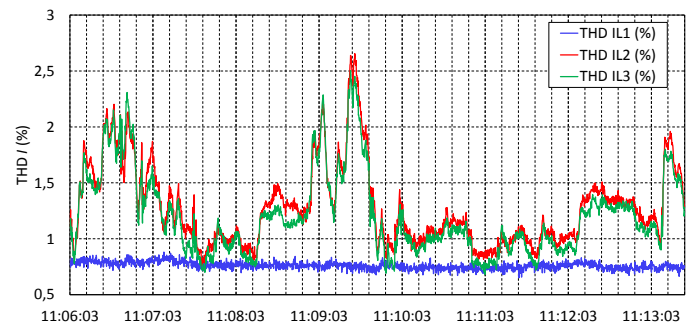


Fig. 21. Current total harmonic distortion on 110 kV side

D. Measurement of unbalance and flicker

Unbalance and flicker were measured on 110 kV level. The measurements were performed during two drives, each lasting 7 minutes. The drives were regulated according to the measuring requirements with frequent acceleration and braking periods.

For the period depicted in Fig. 3, the values of voltage (Fig. 22) and current unbalance (Fig. 23) were obtained at connection point of overhead line 2. Unbalance is determined as the percentage ratio of negative sequence voltage to positive sequence voltage. Also, the values of short time flicker are presented in Table IV.



Fig. 22. Voltage unbalance on 110 kV side

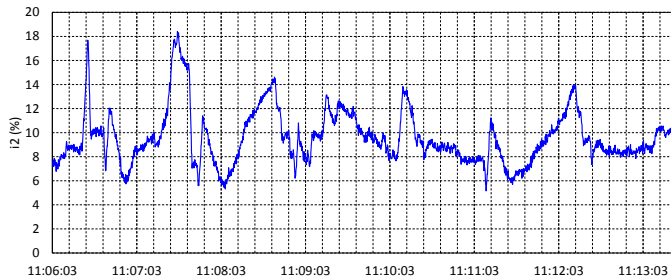


Fig. 23. Current unbalance on 110 kV side

Voltage and current unbalance at connection point of electric railway to transmission network were lower than 3.8 % and 19 % respectively. In order to determine the influence of traction vehicle on unbalance in 110 kV network, measurements should be performed during the one week according to [15]. 95 % of the ten minute mean r.m.s. values of the negative phase sequences should be under 2%.

Short time flicker values per phases are given in Table III. Considering the maximal permitted values defined in standards, measured values of short time flicker were below limits [16].

TABLE III
SHORT TIME FLICKER VALUES ON 110 kV SIDE

Phase	P_{st}
L1	0.1090
L2	0.1046
L3	0.1042

V. CONCLUSIONS

In this paper, the monitoring of power quality parameters at the point of electric railway system connection to transmission system was described. The operation of the electric traction system 25 kV, 50 Hz supplied from traction substation 110/25 kV was presented. Impact of 3f traction motors on transmission network by the measurements of power quality parameters (THD, unbalance, flicker) was investigated.

Railway system with traction vehicle equipped with 3f induction motor was developed in ATP. Waveforms of voltage

and supply current were analyzed. In the calculations the 41st and 42nd harmonics of power frequency was identified with the highest magnitude while in the measurements 3rd, 21st, and 53rd harmonic were significant. That mostly depends on the converters characteristics.

Voltage and current waveforms were analyzed during three operation modes of electric traction vehicle: acceleration, constant drive and regenerative braking. It is clear that 3f traction induction motors have an impact on power quality parameters especially during acceleration and braking. However, operation in energy recovery mode results with the most significant impact.

The values of THD, unbalance and flicker obtained by measurements were below limits prescribed in standards. From the standpoint of power quality and energy consumption efficiency, 3f induction motors in electric traction system have many advantages and their use is increasing.

VI. ACKNOWLEDGMENT

The authors gratefully acknowledge the contributions of the Croatian Transmission System Operator Ltd. and HŽ Infrastruktura Ltd. for enabling the measurements.

VII. REFERENCES

- [1] S. Frey, "Railway electrification Systems & Engineering" White World Publications, Delhi, 2012
- [2] I. Uglešić, M. Mandić, "Napajanje električne vuče", Graphis, Zagreb, 2014.
- [3] Y. Osura, Y. Mochinaga, H. Nagasawa, "Railway Electric Power Feeding Systems", *Japan Railway & Transport Review*, Vol. 16, June 1998
- [4] R. C. Dugan, M. F. McGranaghan, S. Santoso, H. Wayne Beaty, "Electric Power Systems Quality", McGraw-Hill, Third edition, 2012
- [5] B. Milešević, "Electromagnetic influence of electric railway system on metallic structures", Ph.D. dissertation, University of Zagreb, 2014
- [6] T. Achour, M. Pietrzak-David, M. Grandpierre, "Service Community of an Induction Machine Railway Traction System", XIX Int. conference on Electric Machines - ICEM, Rome, 2010
- [7] International Telecommunication Union, "Directives concerning the protection of telecommunication lines against harmful effects from electric power and electrified railway lines" Vol. IV, Geneva, 1989
- [8] A. Zupan, A. Tomasovic Teklic, B. Filipovic-Grcic, "Modeling of 25 kV Electric Railway System for Power Quality Studies", EuroCon 2013, Zagreb, 2013
- [9] W. Buchberger, Die neue schnellfahrende Mahrsystem – Hochleistungslok 1216 der OBB, September 2004, <http://www.br146.de/SiemensPdf/Rh1216-oebb.pdf>, January 2014
- [10] IEEE Standard Association, IEEE Recommendation Practice and Requirements for Harmonic Control in Electric Power Systems, IEEE Std 519™-2014, New Yourk, 2014
- [11] N. Cho, "Allocation of Individual Harmonic Emission Limits in Accordance with the Principles of IEC/TR 61000-3-6", Ph.D. dissertation, Georgia Institute of Technology, 2013
- [12] FAG Wheelset Bearings in the High-Power Locomotive "TAURUS", Examples of Application Engineering Publ. No. WL 07 510 EA, http://www.schaeffler.com/remotemedien/media/_shared_media/08_media_library/01_publications/schaeffler_2/publication/downloads_18/wl_07510_de_en.pdf, January 2015
- [13] Siemens AG Transportation Systems, Electric locomotives, https://www.swe.siemens.com/italy/web/IC/RL/Locomotive/Documents/CP-Trasporti/PSS/ElectricLoco_en.pdf, January 2014
- [14] L. Liudvinavicius, L. P. Lingaitis, Energy Management Systems – Management of Locomotive Tractive Energy Resources, InTech,

August, 2011

- [15] EN 50160:2010, Voltage characteristics of electricity supplied by public electricity networks
- [16] M. H. Albadi, A. S. Hinai, A. H. Al-Badi, M. S. Al Riyami, S. M. Hinai, R. S. Al Abri, "*Measurements and Evaluation of Flicker in High Voltage Networks*", Int. Conference on Renewable Energies and Power Quality, Cordoba, Spain, April 2014